EasyChair Preprint

№ 1506

Autonomous Driving of Six-Wheeled Dump Truck with Retrofitted Robot

Tomohiro Komatsu, Yota Konno, Seiga Kiribayashi,
Keiji Nagatani, Takahiro Suzuki, Kazunori Ohno, Taro Suzuki,
Naoto Miyamoto, Yukinori Shibata and Kimitaka Asano

September 12, 2019

Autonomous Driving of Six-Wheeled Dump Truck with Retrofitted Robot

Tomohiro Komatsu, Yota Konno, Seiga Kiribayashi, Keiji Nagatani, Takahiro Suzuki, Kazunori Ohno, Taro Suzuki, Naoto Miyamoto, Yukinori Shibata, and Kimitaka Asano

Abstract In Japan, expectations for the automation of construction machines are increasing to solve labor shortage in the construction industry. In this research, a robotization method by retrofitting a robot to conventional construction machines is introduced to lower the introduction barrier for regional construction companies. The target machine is a six-wheeled dump truck. With a retrofitted internal sensor unit and derived kinematics of six-wheeled articulated dump truck, a conventional Global Navigation Satellite System (GNSS)-based path tracking method was implemented on it. In addition, to ensure safety during operation, an emergency stop function was installed on the dump truck with three-dimensional Light Detection and Ranging (3D LiDAR). Initial experiments of forward and backward path tracking with an actual dump truck confirmed the validity of the method, and the maximum tracking error was 1 m. Further, in an emergency stop experiment, the dump truck detected the obstacle and stopped immediately after obstacle detection within the emergency-stop region, i.e., 25 m x 3 m in front of the dump truck. Based on the initial experiments, the authors concluded that even the retrofitted conventional

Tomohiro Komatsu (Tohoku University/ Kowatech Co., Ltd.), Yota Konno, Seiga Kiribayashi, Takahiro Suzuki (Tohoku University), Kazunori Ohno (Tohoku University/ RIKEN AIP), and Naoto Miyamoto (Tohoku University)
Tohoku University, 6-6-10, Aramaki-Aoba, Sendai, Japan, e-mail: komatsu@frl.mech.tohoku.ac.jp
Kowatech Co., Ltd., 5-18-18, Samukawa-Ichinomiya, Kozagun, Kanagawa, Japan.

Keiji Nagatani
The University of Tokyo, 7-3-1 Hongo, Bunkyo-ku, Tokyo, Japan.

Taro Suzuki
Chiba Institute of Technology, 2-17-1 Tsudanuma, Narashino, Chiba, Japan.

Yukinori Shibata
Sato Koumuten Co., Ltd., 69, Kami-Nagadan, Kamigun, Miyagi, Japan.

Kimitaka Asano
Sanyo-Technics Co., Ltd., 3-1-40, Nigatake, Sendai, Miyagi, Japan.

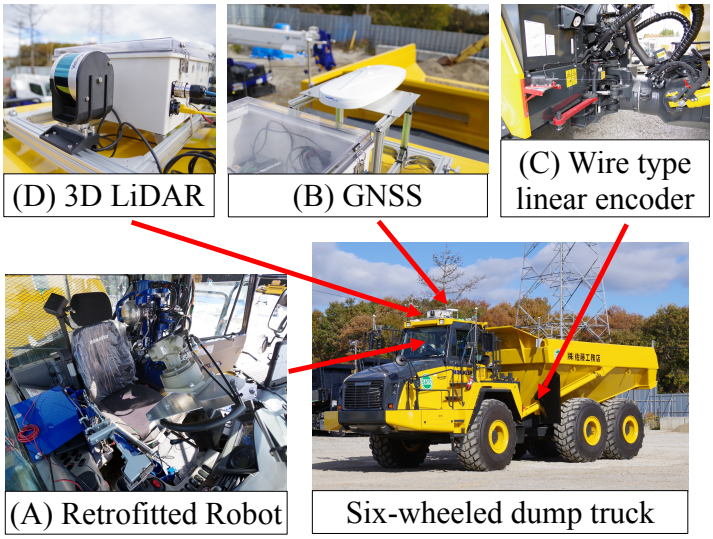

Fig. 1 Six-wheeled dump truck and equipment for autonomous driving.

dump truck could perform basic functions for autonomous driving, such as path tracking and emergency stop.

1 Introduction

Currently, the declining birthrate and aging population have become social problems in Japan. In the construction industry, this problem is serious and labor shortage due to aging will occur. Therefore, expectations for autonomous construction machines are increasing. Currently, in Japan, promoting the automation of construction machinery is a national policy. The Ministry of Land, Infrastructure, Transport and Tourism (MLIT) has established policies such as information construction and i-Construction [1]. According to the above background, major construction machine manufacturers and major construction companies are researching and developing the automation of construction machinery [2], [3]. However, in local companies, only a few cases exist where autonomous construction machines, or smart construction machine, are introduced to regional construction companies.

Therefore, the authors aim to realize automated construction machines owned by regional construction companies. Particularly, in this research, the target is a 30-ton six-wheeled dump truck. The task to realize is earth and sand transportation from a certain loading position to an unloading position. This article reports an examination of functions required for the autonomous driving of the existing six-wheeled dump trucks, development of control modules, and verification using an actual truck with the modules. It includes the following four topics:

1. development of robotic control module for conventional dump truck,
2. development of in-vehicle sensor modules according to vehicle characteristics,
3. construction of control system to integrate the above and derivation of kinematics for a six-wheeled dump truck, and
4. consideration of a method to detect obstacles with three-dimensional (3D) Light Detection and Ranging (LiDAR).

The effectiveness of the above was confirmed by initial experiments on an actual 30-ton dump truck.

2 Robotization of existing six-wheeled dump truck

This research aims to realize autonomous driving for conventional six-wheeled dump trucks owned by regional construction companies. The target task for the dump trucks is earth and sand transportation from a certain loading position to an unloading position. Functions to realize autonomous driving are classified into the following four categories:

- Vehicle operation to handle steering wheel, accelerator, and brake
- Acquisition of vehicle information for vehicle control such as speed and position of a dump truck
- Acquisition of environmental information to recognize surrounding environments such as obstacles and driving road surface
- Control system to integrate the above functions

The authors' approaches to realize the above functions are introduced in the following subsections.

2.1 Development of retrofitted robot: SAM

To realize the functions for the vehicle operation of dump trucks, it is necessary to handle the steering wheel, accelerator, and brake pedal. Some methods can be used to operate a vehicle directly by controlling its hydraulic system or electric signals such as CAN communication [4], [5]. However, it is difficult because vehicle information is not disclosed by construction companies, typically.

Therefore, in this research, a robot is retrofitted to the vehicle to physically drive the dump truck. Consequently, a significant modification of the vehicle is not required, and the robot can be developed by the physical vehicle information. In this paper, the development of a robot on the driver's sheet, particularly to enable the operations of steering, accelerator, and the brake pedal, is focused in the following.

Fig.1(A) shows the robot, called SAM. SAM is commercialized as a retrofitted system that enables the remote control of an existing hydraulic excavator [6], [7]. In this research, we reconfigured a commercialized SAM to control a dump truck.

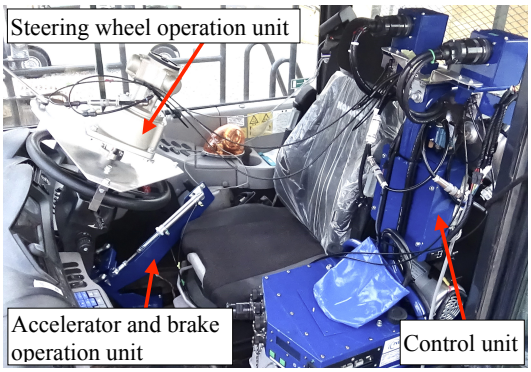

Fig. 2 Retrofitted robot, SAM, which is located in passenger's seat.

SAM includes a pneumatic servo system that exhibits mechanical compliance from the compressibility of air such that it is considered effective against disturbances such as vibration and shock to construction machines. In field experiments, as shown in section 4, the main body of SAM was installed on the passenger seat such that the person in the driver's seat can operate the brake for an emergency stop.

2.1.1 Operation unit for the steering wheel

In the steering of the six-wheeled dump truck, the articulated angle changes according to the amount of rotation of the steering wheel. However, the neutral position of the steering is not constant. This is because the control amount of the steering wheel is that of the hydraulic pressure that controls the articulation mechanism, and not the articulation angle itself. In addition, the handle is structured to rotate infinitely. Therefore, a radial piston air motor with no limit in rotation range was adopted for the steering wheel operation. The air motor is operated by compressed air; therefore, it is resistant to overloads and external impacts during steering. In the steering drive mechanism, an air motor installed at the top of the steering wheel rotates the steering shaft directly. The rotational speed can be controlled by changing the air flow rate of the air motor.

2.1.2 Operation unit for accelerator and brake pedals

The vehicle speed of a six-wheeled dump truck is controlled by the amount of depression of the accelerator and brake pedals. Therefore, a pneumatic servo system was built on the pneumatic cylinder for the operation of the accelerator and brake pedal. For safety reasons, when all the power in the system is lost, the air in the

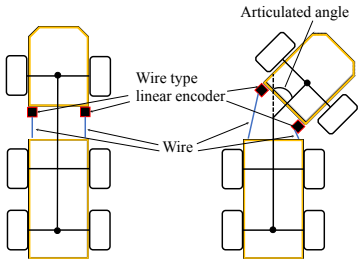

Fig. 3 Schematic diagram of the measurement method of bending angle.

cylinder is exhausted, and the spring-push-type pneumatic cylinder is configured to depress the brake pedal automatically.

2.2 Sensing unit for acquisition of vehicle status

In recent dump trucks, their speed and steering angle are measured in the system. However, practically, it is difficult to obtain information for researchers/operators because it is not disclosed. Therefore, the authors developed a sensor unit that obtains the position, heading, and articulated angle of the vehicle, and can be installed easily on the dump truck.

Fig.1(B) shows the GNSS unit (manufactured by Hemisphere: ssV-102) [8]. The system is equipped with two GNSS such that it acquires the position and heading of the dump truck. Further, the velocity of the vehicle is calculated from the difference between the measured positions and times. The GNSS was located at the center of the front wheel shaft of the vehicle.

To acquire the articulate angle, which is equivalent to the steering angle, a wire-type linear encoder (manufactured by MUTOH: DE-04-C)[9] was used, as shown in Fig.1(C). Fig.3 shows a schematic diagram of the measurement method of bending angle. From the measurement results, it was confirmed that there was linearity between the wire length obtained by the linear encoder and the articulated angle. However, since the wire-type sensor is not reliable enough for operation at construction sites such as rocky or dirt environments, it is assumed to be a tentative method. Another better method, e.g. using laser range sensor, will be replaced in the future.

2.3 Path tracking method for six-wheeled dump truck

To realize the autonomous driving of a dump truck that does not collide with obstacles, path planning is important. In this study, it is assumed that the path is

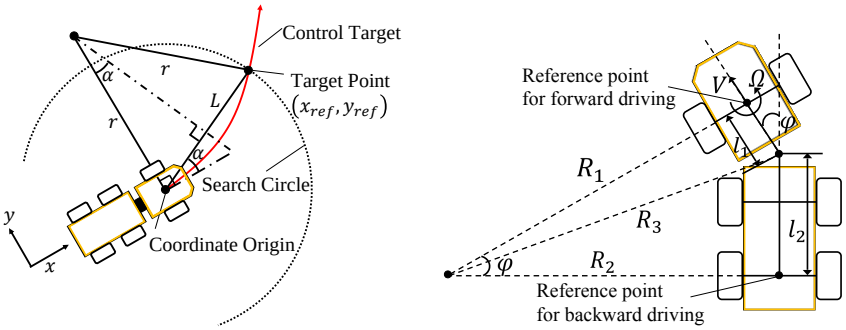

(a) Conceptual diagram of pure pursuit method

(b) Flexion of six-wheeled dump truck.

Fig. 4 Path planning method.

planned, and mainly the method of path tracking control is focused. The path tracking method, which the authors chose in this project, is Pure Pursuit method [10], [11] applied to autonomous vehicles for an easy gain tuning.

Fig.4(a) shows the conceptual diagram of the pure pursuit path tracking algorithm. The target point is determined from the current vehicle velocity V and a gain parameter d. The radius of the circle to search for the target point from the current position is expressed as follows:

$$L = Vd \tag{1}$$

The angle α between a straight line passing through the target point (x_{ref}, y_{ref}) and the current position (= coordinate origin) and the heading line of the vehicle is expressed as follows:

$$\alpha = \tan^{-1}\left(\frac{y_{ref}}{x_{ref}}\right). \tag{2}$$

The reference path is generated as a tangential line to the current vehicle heading and passes through both the target point and current position. Subsequently, the rotation radius of the vehicle r is expressed as the following equation from geometric relationships:

$$r = \frac{L}{2\sin\alpha}. \tag{3}$$

Therefore, the reference rotational velocity of the vehicle Ω_{ref} is expressed as follows:

$$\Omega_{ref} = \frac{V}{r} = \frac{2V\sin\alpha}{L}. \tag{4}$$

2.3.1 Kinematics of the six-wheeled dump truck

The kinematics of the six-wheeled dump truck was derived to calculate the rotational velocity, which is the operation input for a vehicle, from the articulated angle of the vehicle. Fig.4(b) shows the kinematics of the six-wheeled dump truck. The geometrical relationship of the vehicle is expressed as follows:

$$R_1^2 + l_1^2 = R_2^2 + l_2^2 = R_3^2, \tag{5}$$

$$R_2 = R_1 \cos\varphi + l_1 \sin\varphi, \tag{6}$$

where R_1 denotes the length between the center of the front axle and the rotational center; R_2 the length between the center of the rear axle and the rotational center; R_3 the length between the hinge point and rotational center; l_1 the length between the front axle and hinge point; l_2 the length between the rear axle and hinge point; and φ the articulated angle.

According to equations 5 and 6, R_1 is expressed as follows:

$$R_1 = \frac{l_1 \cos\varphi + l_2}{\sin\varphi}. \tag{7}$$

Then, the rotational velocity Ω_{now} is expressed as follows:

$$\Omega_{now} = \frac{V}{R_1} = \frac{V \sin\varphi}{l_1 \cos\varphi + l_2}. \tag{8}$$

Thus, the relationship between the rotational velocity and the articulated angle of the six-wheeled dump truck is derived. Therefore, the values for vehicle control are obtained by the kinematics.

2.3.2 Forward and backward path tracking

In the target task, for transporting soil from the loading position to the unloading position, both forward and backward driving are required for a dump truck. In forward driving, the center of the front wheel shaft is defined as a reference point. However, in backward driving, the center of the rear wheel shaft of the vehicle is regarded as the reference point. This reference point is regarded as the current position of the vehicle in Pure Pursuit method. The position and heading of the rear wheel center are derived using the position and heading of the GNSS, articulate joint angle, length l_1, and length l_2.

3 Obstacle detection

3.1 Acquisition function of environmental information based on 3D LiDAR

For the safe driving of an autonomous dump truck, it is necessary to confirm the condition of the road surface and the existence of obstacles. Acquiring a 3D topography map and updating the map is effective to enable the above. Therefore, a 3D LiDAR is typically used to acquire environmental information [12],[13]. In this research, a safety function based on the 3D LiDAR is introduced to confirm the safety in front of the dump truck where human entry cannot be completely restricted in a relatively common construction site.

First, a suitable installation configuration of the 3D LiDAR is examined for the six-wheeled dump truck and the driving environment in construction sites. Next, an algorithm for obstacle detection with the LiDAR was implemented. In the initial examination, verification of the forward obstacle detection was carried out, and rear obstacle detection is in future works.

3.2 Examination of suitable installation configuration of 3D LiDAR

In this research, the device to obtain environmental information is the 3D LiDAR, manufactured by Velodyne (VLP-16) [14]. Fig.1(D) shows the LiDAR installed on the vehicle. Obstacles are detected as point cloud data acquired from the 3D LiDAR. In the measurement range of the 3D LiDAR, 16 lasers are emitted at intervals of 2° in the vertical direction, and the measurement range is 30°. In the horizontal direction, the laser is emitted at an interval of 0.2° in all directions. The LiDAR was installed on the roof because the front can be sufficiently overlooked without being affected by the road surface irregularities and it can be easily detached. Typically, the LiDAR (VLP-16) is installed horizontally to obtain the environmental information of all surroundings. However, in this research, the installation direction of the LiDAR was vertical to increase the resolution of the traveling direction.

3.3 Derivation of unmeasurable region

To confirm the limitation of the measurement region when LiDAR is placed vertically, the unmeasurable region is calculated geometrically from the positional relationship between the LiDAR and ground. Fig.5(a) shows the measurement of obstacles from the road surface upwards. Here, h m denotes the installation height of the LiDAR from the ground; h_{obs} m the height of the measurable obstacle; θ° the angle

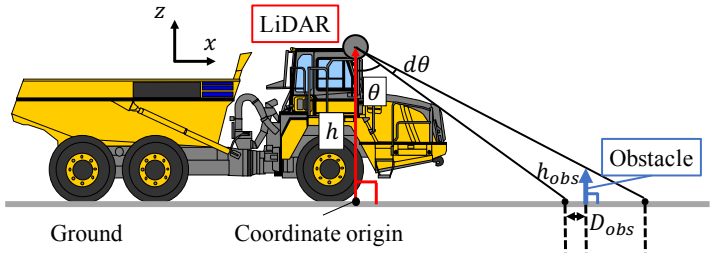

(a) Diagram of positional relationship between 3D LiDAR installed in dump truck and obstacle.

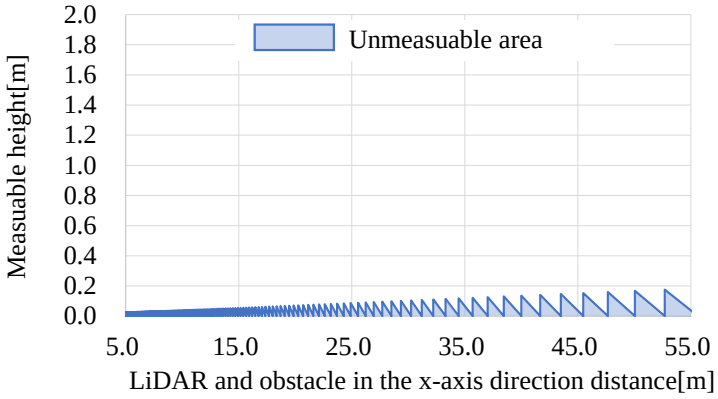

(b) Graph of unmeasurable region.

Fig. 5 Diagram of LiDAR installation position and unmeasured area.

between the perpendicular drawn from the LiDAR to the ground and the straight line of the emitted laser; $d\theta^\circ$ the angular resolution of the LiDAR; and D_{obs} m the distance between the point at which the emitted laser crosses the ground and the obstacle in the x-axis direction. From the triangle approximation, the height of the detectable obstacle h_{obs} is expressed as follows:

$$h : h\tan(\theta + d\theta) = h_{obs} : h\tan(\theta + d\theta) - h\tan\theta - D_{obs} \tag{9}$$

$$h_{obs} = \frac{h\tan(\theta + d\theta) - h\tan\theta - D_{obs}}{\tan(\theta + d\theta)}. \tag{10}$$

The parameters in this verification test are $h = 3.5$ m, $d\theta = 0.2^\circ$. Fig. 5(b) shows an unmeasurable region calculated from the measurable height. The unmeasurable height is approximately 0.2 m at 50 m.

3.4 Obstacle detection method

In this research, for a simple and robust obstacle detection, an obstacle is assumed if the gap dz in the z-axis direction between adjacent point cloud data is larger than the threshold dz_{th}. The calculation is performed independently for each of the 16 lasers to be emitted. In the lateral direction, each laser gap is the minimum recognition width. For example, at the point of 10 m from laser range finder, minimum recognition width is 0.35 m. Because this method involves a simple comparison of height between two points, it is effective for long objects such as people and signboards targeted in this verification.

4 Initial field experiments

To confirm the effectiveness of the proposed method, two initial field experiments were conducted using the developed device and an articulated dump truck.

Both experiments were conducted in Sato Koumuten's field in Kami-gun, Miyagi prefecture. The environment was a flat surface. The target vehicle in both experiments was HM300-5 (manufactured by Komatsu)[15]. The details are introduced in the following subsections.

4.1 Experiments of forward and backward path tracking

4.1.1 Purpose of experiment and conditions

In this experiment, the performance of the path tracking system shown in section 2 is evaluated by comparing the error between the reference path and the executed path. The reference path of the dump truck, which is a list of GNSS coordinates, was generated by manually driving the vehicle in advance. The translational reference velocity was 6 km/h for forward path tracking and 4 km/h for backward path tracking. The distance from the current position obtained by GNSS to the closest point on the reference path is defined as the tracking error. In this experiment, the gain parameter d was determined by trial and error.

4.1.2 Experimental results and discussions

Figures 6(a) and 6(b) show the experimental results of forward and backward path tracking. The starting point is the coordinate origin$(0,0)$. The dotted line is the reference path, and the solid line is the path trajectory estimated by the GNSS.

Based on Fig.6(a), the maximum error between the reference path and the actual path was 0.5 m for forward path tracking. However, based on fig.6(b), the maximum

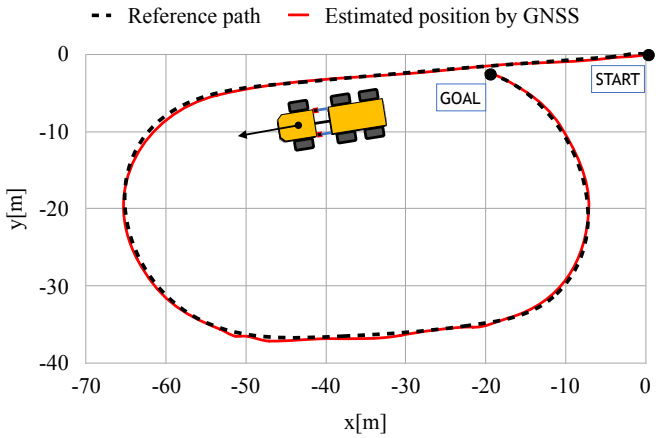

(a) Experiment results of forward path tracking.

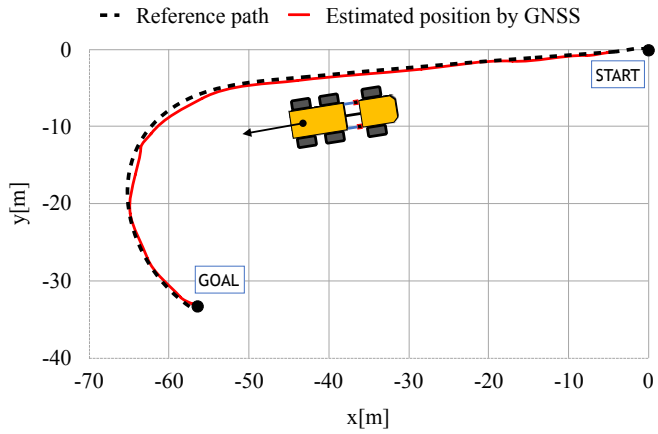

(b) Experiment results of backward path tracking.

Fig. 6 Results of autonomous path tracking experiment.

error between the reference path and the actual path was 1.0 m for backward path tracking.

The magnitude of the error is considered to be within the acceptable range. However, the error between the target path and the actual trajectory for backward path tracking was larger than that for forward path tracking. The reason is as follows. In backward path tracking, the (x, y) position of the origin of the dump truck is located at the middle of the rear wheels. The position is calculated by the position of the

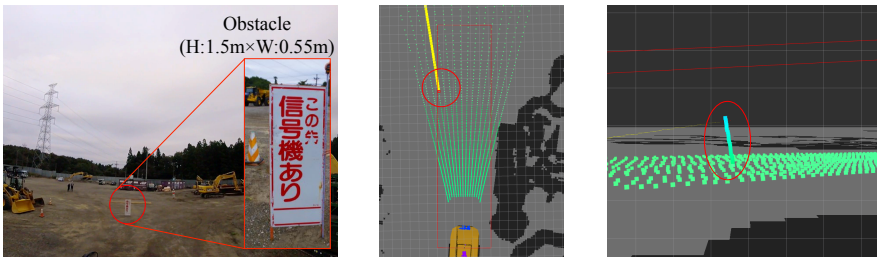

(a) Camera image. (b) Measurement screen. (c) Measurement screen enlarged with changing viewpoint.

Fig. 7 Obstacle detection result in case of emergency stop.

GNSS installed on the front roof of the dump truck and the bending angle of the articulate mechanism. The measurement of the articulate angle is now performed by wire linear encoders, but includes errors. Therefore, the angular error affects the positioning error of the origin of the dump truck in backward path tracking.

4.2 Emergency stop experiment by detection of obstacles

4.2.1 Purpose of experiment and conditions

To realize the safe driving of the six-wheeled dump truck, an obstacle detection, as shown in section 3.4, and an emergency stop function were implemented. The purpose of the experiment is to confirm whether the simple proposed method operates correctly in a real field with a real dump truck.

The LiDAR was installed at the top of the roof of the driver's seat. The height was 3.6 m from the ground. The target obstacle was a signboard of a construction site with a height of 1.5 m and width of 0.55 m. The translational reference speed of the dump truck was 6 km/h. The threshold dz_{th} was set to 0.7 m. In this experiment, a dump truck executed forward path tracking motion on a road where obstacles were placed in advance. The detection region of the obstacles was set as 0 to 25 m in the depth direction and -3 to 3 m along the width of the road, in the horizontal direction from the LiDAR. When an obstacle is detected within this range, the vehicle stops autonomously.

4.2.2 Experimental results

Before the emergency stop experiments, a static capability verification of the 3D LiDAR was conducted. The target obstacle was set 50 m away from the dump truck, and the detection function replied detection of it correctly. Therefore, in considera-

tion of the margin, it was concluded that the system was acceptable for the detection of obstacles within 25 m.

Fig.7 shows the experimental results. The results of the emergency stop experiments are introduced in the following. Fig.7(a) shows the image obtained by the camera installed on the roof of the dump truck, fig.7(b) shows the point cloud data drawn from the top of the vehicle, and fig.7(c) shows the point cloud data drawn from the side of the vehicle. The mesh width of Figs. 7(b) and 7(c) is 1 m. In Fig.7(b), the dotted green line shows the scanning line of the LiDAR, the red frame shows the obstacle detection range, the red circle shows the point where the obstacle is detected, and the solid yellow line shows the scanning line blocked by the obstacle. According to Figs. 7(b) and 7(c), changes due to the obstacles were confirmed in the point cloud data obtained from the LiDAR. Subsequently, the dump truck stopped autonomously as soon as the detected part was located in the obstacle detection range. In addition, it was confirmed that the dump truck also stopped by detection of a human as an obstacle.

Consequently, it was confirmed that the obstacle detection algorithm was operating effectively. However, in the current implementation, the obstacle detection algorithm works excessively for vegetation on the outside of the driving area. In future works, the detection algorithm should work within the driving area of the dump truck.

5 Conclusions

In this research, the authors proposed a method of robotization of a conventional six-wheeled dump truck with simple modifications and performed some initial experiments. This research involved the (1) proposal of a retrofitted control module to robotize a dump truck, (2) development of an internal sensor module to enable path tracking motion by the dump truck, (3) derivation of the six-wheeled dump truck kinematics and implementation of path tracking method, and (4) obstacle detection with a 3D LiDAR.

Based on the initial field experiments, the following results were obtained:

1. It was confirmed that the retrofitted robot operated the accelerator, brake, and steering of the dump truck.
2. The integrated system enabled path tracking motion by vehicle-mounted sensors that detected the vehicle's speed, heading, and articulate angle.
3. Under flat road conditions, the maximum path tracking error was 0.5 m for forward path tracking (6[km/h]) and 1.0 m for backward path tracking (4 km/h).
4. During the autonomous driving (6 km/h) of the dump truck, the obstacle detection method with the 3D LiDAR detected an obstacle (1.5 m high, 0.55 m wide); when the dump truck entered the emergency stop region, the vehicle stopped immediately.

Based on the above, it is possible to perform autonomous driving and enable emergency stop by applying the proposed method to the conventional six-wheeled dump truck.

In future works, to apply the autonomous dump to real construction sites, the authors plan to implement a combination of functions, such as gear change, forward/backward path tracking, and path planner. Further, the performance evaluation of path tracking and obstacle detection in different vehicle speeds are potential future works.

Acknowledgment

This paper is based on the results obtained from a project commissioned by the New Energy and Industrial Technology Development Organization (NEDO).

References

1. Ryou Hashimoto. Promotion Consortium (Special feature: Further promotion of i-construction). *Public works management journal*, No. 469, pp. 8–13, 2017.
2. Dewit Andrew. Komatsu, smart construction, creative destruction, and Japan' s robot revolution. *The Asia-Pacific Journal*, Vol. 13, No. 8, pp. 2–2, 2015.
3. Satoru Miura, Izuru Kuronuma and Kenniti Hamamoto. Next generation construction production system: On automated construction machinery *Civil Engineering Conference in the Asian Region*, 2016.
4. Yuming Yin, Subhash Rakheja and Paul-Emile Boileau. Multi-performance analyses and design optimisation of hydro-pneumatic suspension system for an articulated frame-steered vehicle. *Vehicle system dynamics*, pp.108-133, 2018.
5. Qingyong Meng, Lulu Gao, Heping Xie and Fengqian Dou. Analysis of the Dynamic Modeling Method of Articulated Vehicles. *Journal of Engineering Science and Technology Review*, vol.10, pp.18-27, 2017.
6. Kowatech. Remote steering robot "SAM". http://www.kowatech.co.jp/products/sam.
7. Tomohiro Komatsu and Atsushi Okuyama. Integrated design of pressure and position control systems in pneumatic artificial rubber muscle. *Proceedings of the 58th Japan joint Automatic Control Conference CD-ROM*, 1l3-3, 2015.
8. Hemisphere. ssV-102 smart compass. http://www.hemgps.com/ssv102.html.
9. Mutoh. Linear encoder. https://www.mutoh.co.jp/products/ deji/linearencoder/index.html.
10. R. Craig Coulter. Implementation of the Pure Pursuit Path Tracking Algorithm. *Robotics Institute, Pittsburgh, PA, Tech. Rep. CMU-RI-TR-92-01*, January 1992.
11. Hiroki Ohta, Naoki Akai, Eijiro Takeuchi, Shinpei Kato and Masato Edahiro. Pure pursuit revisited: Field testing of autonomous vehicles in urban areas. *Cyber-Physical Systems, Networks, and Applications (CPSNA), 2016 IEEE 4th International Conference on*, pp. 7–12, 2016.
12. Kuwata, Y., Teo, J., Karaman, S., Fiore, G., Frazzoli, E. and How, J. Motion planning in complex environments using closed-loop prediction. *In AIAA Guidance,Navigation and Control Conference and Exhibit*,2008.
13. Erke Shang, Xiangjing An, Tao Wu, Tingbo Hu, Qiping Yuan, and Hangen He. Lidar based negative obstacle detection for field autonomous land vehicles. *Journal of Field Robotics*, Vol. 33, No. 5, pp. 591–617, 2016.
14. Velodyne LiDAR. Puck, vlp-16. https://velodynelidar.com/vlp-16.html.
15. Komatsu. HM300-5. https://www.komatsu.eu/en/dump-trucks/articulated-dump-trucks/hm300-5.